

# Constraints on the MSSM from the Higgs Sector

## A pMSSM Study of Higgs Searches, $B_s^0 \rightarrow \mu^+ \mu^-$ and Dark Matter Direct Detection

A. Arbey<sup>123</sup>, M. Battaglia<sup>245</sup> and F. Mahmoudi<sup>26</sup>

<sup>1</sup> Université de Lyon, France; Université Lyon 1, CNRS/IN2P3, UMR5822 IPNL, F-69622 Villeurbanne Cedex, France

<sup>2</sup> CERN, CH-1211 Geneva 23, Switzerland

<sup>3</sup> Observatoire de Lyon, CNRS, UMR 5574; Ecole Normale Supérieure de Lyon, F-69561 Saint-Genis Laval Cedex, France

<sup>4</sup> Santa Cruz Institute of Particle Physics, University of California, Santa Cruz, CA 95064, USA

<sup>5</sup> Lawrence Berkeley National Laboratory, Berkeley, CA 94720, USA

<sup>6</sup> Clermont Université, Université Blaise Pascal, CNRS/IN2P3, LPC, BP 10448, 63000 Clermont-Ferrand, France

**Abstract.** We discuss the constraints on Supersymmetry in the Higgs sector arising from LHC searches, rare  $B$  decays and dark matter direct detection experiments. We show that constraints derived on the mass of the lightest  $h^0$  and the CP-odd  $A^0$  bosons from these searches are covering a larger fraction of the SUSY parameter space compared to searches for strongly interacting supersymmetric particle partners. We discuss the implications of a mass determination for the lightest Higgs boson in the range  $123 < M_h < 127$  GeV, inspired by the intriguing hints reported by the ATLAS and CMS collaborations, as well as those of a non-observation of the lightest Higgs boson for MSSM scenarios not excluded at the end of 2012 by LHC and direct dark matter searches and their implications on LHC SUSY searches.

**PACS.** 11.30.Pb Supersymmetry – 12.60.Jv Supersymmetric models – 14.80.Da supersymmetric Higgs bosons

## 1 Introduction

The search for Supersymmetry (SUSY) is the main focus of the studies of physics beyond the Standard Model (SM) at the LHC. Having acquired the status of possibly the best motivated theory of new physics over the past decades, Supersymmetry in its minimal incarnation (MSSM) with R-parity conservation is widely regarded as the template for theories and models with a conserved quantum number, leading to a candidate for relic dark matter and distinctive experimental signatures with hadrons, leptons and missing transverse energy,  $MET$ .

In view of the negative results of the searches in channels with  $MET$  conducted by the ATLAS and CMS experiments on more than  $1 \text{ fb}^{-1}$  of statistics at 7 TeV [1–5], questions on the continuing viability of the MSSM have arisen. These have been driven in particular by the strong impact of the LHC exclusion bounds on highly constrained MSSM models, such as the CMSSM and mSUGRA with few free parameters. Studies considering more general models without implicit correlations between the masses of the supersymmetric particle partners, such as the 19-parameter phenomenological MSSM (pMSSM), have demonstrated that a wide phase space of solutions, compatible with flavour physics, low energy data and dark matter constraints and beyond the current sensitivity of the LHC experiments, exists [6–8]. Even at the end of the current LHC run, with an anticipated integrated luminosity of or-

der of  $15 \text{ fb}^{-1}$  per experiment, many of these solutions will not be tested. These solutions are compatible with all present bounds and  $\sim 30\%$  of them have values of the fine tuning parameter, according to the definition of Ref. [9], below 100. This will make not possible to falsify the MSSM as the model of new physics beyond the SM and the source of relic dark matter in the universe, if no missing  $E_T$  signal will be observed at the LHC by the end of 2012.

However, there is an alternative path to tightly constrain and test the MSSM at the LHC, which involves the bounds on its Higgs sector. Searches for the Higgs boson are expected to either discover or exclude a SM-like neutral Higgs boson with mass in the range  $114 < M_H < 127$  GeV, which represents the current combined LEP and LHC mass bounds [10–12] and corresponds to the mass range expected for the MSSM light Higgs boson,  $h^0$ , as well as that indicated by electro-weak data for a SM-like boson,  $H_{SM}^0$ . Presently, both ATLAS and CMS have a sensitivity to a light neutral Higgs boson in this mass range comparable to production yields expected in the SM. In the MSSM, the  $h^0$  mass depends on radiative corrections generated by SUSY loops and its couplings can be shifted resulting in a suppression (or an enhancement) of the production cross sections and decay branching fractions for the channels most relevant for the results of the LHC Higgs searches, compared to the SM predictions. However, such a suppression implies phenomenology which can be stud-

ied or constrained in direct SUSY searches and in rare  $B$  decays at the LHC as well as in direct dark matter detection experiments, by the end of 2012.

In this paper we discuss these constraints and their implications on the MSSM from a study of the pMSSM with 19 free parameters [13], where we assume that the lightest neutralino,  $\chi_1^0$  is the lightest supersymmetric particle (LSP). We further assume that the neutralino LSP is the weakly interacting massive particle (WIMP) responsible for (at least part of) the dark matter in the universe and focus on two scenarios for the light  $h^0$ . First, we consider a light Higgs boson with  $123 < M_{h^0} < 127$  GeV, as possibly suggested by the intriguing hints in the preliminary results of the Higgs searches at the LHC with almost  $5 \text{ fb}^{-1}$  of data [10–12]. Then, we consider the exclusion of the Higgs boson to a rate three times below that predicted in the SM, by the end of 2012. This paper is organised as follows. In section 2 we summarise the dependence of the Higgs mass and of the mechanisms of suppression of Higgs event yield at the LHC on the MSSM parameters, while section 3 investigates the present and projected bounds from LHC and DM experiments. We present the scenarios compatible with these bounds in section 4, while section 5 has the conclusions.

## 2 SUSY Higgs bosons and pMSSM scans

The calculation of the lightest Higgs boson mass,  $M_{h^0}$ , in the MSSM is the most precise prediction for a particle in the SUSY theory. After accounting for radiative corrections,  $M_{h^0} \lesssim 135$  GeV [14–16]. It is tantalising that this bound falls in the mass range indicated by electro-weak fits and within the window left open by Higgs searches at LEP-2, Tevatron and the LHC. This makes its search the most readily available method to either confirm or falsify a firm SUSY prediction. While the discovery of a Higgs-like particle in this mass range would also be compatible with the SM only, without any SUSY extension, and its exclusion could be reconciled with the SM, the exclusion of the Higgs boson in this range would put an end to the MSSM as viable extension of the SM. At the same time the determination of the lightest Higgs mass would provide us with constraints on the MSSM parameters. In particular, a value of  $M_h$  around 125 GeV either rules out, or severely constrains, several scenarios so far extensively used in the study of Supersymmetry, such as the so-called “no-mixing” and “typical-mixing” scenarios [17].

In order to study the properties of SUSY Higgs bosons, we perform a flat scans of the pMSSM, where we vary its 19 parameters in an uncorrelated way within the ranges given in Table 1, and generate a total of 40M points. The scan range is explicitly chosen to include the so-called “maximal mixing” region [18], at  $X_t \sim \sqrt{6}M_{\text{SUSY}}$ , where  $X_t = A_t - \mu \cot \beta$  and  $M_{\text{SUSY}} = \sqrt{m_{\tilde{t}_1} m_{\tilde{t}_2}}$ , which corresponds to larger values of  $M_{h^0}$ . We select the set of points fulfilling constraints from flavour physics and lower energy searches at LEP-2 and the Tevatron, as discussed in [8]. We find  $65 < M_{h^0} < 143$  GeV for points compatible with those constraints. In addition, we perform dedi-

Parameter	Range
$\tan \beta$	[1, 60]
$M_A$	[50, 2000]
$M_1$	[-2500, 2500]
$M_2$	[-2500, 2500]
$M_3$	[50, 2500]
$A_d = A_s = A_b$	[-10000, 10000]
$A_u = A_c = A_t$	[-10000, 10000]
$A_e = A_\mu = A_\tau$	[-10000, 10000]
$\mu$	[-3000, 3000]
$M_{\tilde{e}_L} = M_{\tilde{\mu}_L}$	[50, 2500]
$M_{\tilde{e}_R} = M_{\tilde{\mu}_R}$	[50, 2500]
$M_{\tilde{\tau}_L}$	[50, 2500]
$M_{\tilde{\tau}_R}$	[50, 2500]
$M_{\tilde{q}_{1L}} = M_{\tilde{q}_{2L}}$	[50, 2500]
$M_{\tilde{q}_{3L}}$	[50, 2500]
$M_{\tilde{u}_R} = M_{\tilde{c}_R}$	[50, 2500]
$M_{\tilde{t}_R}$	[50, 2500]
$M_{\tilde{d}_R} = M_{\tilde{s}_R}$	[50, 2500]
$M_{\tilde{b}_R}$	[50, 2500]

**Table 1.** pMSSM parameter ranges adopted in the scans (in GeV when applicable).

cated scans for specific scenarios yielding large suppression of the Higgs production and decay channels explored at the LHC, where we restrict the ranges of a subset of the pMSSM parameters, as discussed in section 3.

The details of the pMSSM scans and the tools used for the computations of the spectra and relevant observables have been presented in details elsewhere [8]. Here we mention only those most relevant to this study. SUSY mass spectra are generated with `SOFTSUSY 3.2.3` [19]. The decay branching fractions of Higgs bosons are obtained using `HDECAY 4.40` [20] including gaugino and sfermion loop corrections, and cross-checked with `FeynHiggs 2.8.5` [21, 22]. The widths and decay branching fractions of the other SUSY particles are computed using `SDECAY 1.3` [23]. The dark matter relic density is calculated with `SuperIso Relic v3.2` [24–26], which provides us also with the flavour observables. The neutralino-nucleon scattering cross-sections are computed with `micrOMEGAs 2.4` [27]. The  $gg$  and  $bb$  Higgs production cross sections are computed using `HIGLU 1.2` [28, 29] and `FeynHiggs 2.8.5`, respectively. The Higgs production cross sections and the branching fractions for decays into  $\gamma\gamma$  and  $WW, ZZ$  from `HIGLU` and `HDECAY` are compared to those predicted by `FeynHiggs`. In the SM both the  $gg \rightarrow H_{SM}^0$  cross section and the branching fractions agree within  $\sim 3\%$ . Significant differences are observed in the SUSY case, with `HDECAY` giving values of the branching fractions to  $\gamma\gamma$  and  $WW, ZZ$  which are on average 9% lower and 19% larger than those of `FeynHiggs` and have an r.m.s. spread of the distribution of the relative difference between the two programs of 18% and 24%, respectively. In the following, we use `HDECAY` throughout the analysis and we comment on the effects of using the results of `FeynHiggs` instead at the end of section 4.1. Then, we test the sensitivity to the  $b$ -quark mass by vary-

ing the  $b$  pole mass by  $\pm 200$  MeV. The corresponding relative change of the SUSY to SM ratio of the branching fractions is  $\pm 0.1\%$  for both  $\gamma\gamma$  and  $WW/ZZ$  decays. Finally, we test the decoupling limit by taking the ratio of the SUSY branching fractions to their SM counterparts for  $M_A > 700$  GeV for HDECAY. We find  $0.994 \pm 0.005$  and  $0.954 \pm 0.005$  for  $\gamma\gamma$  and  $WW/ZZ$ . For computing the ratio of the  $\gamma\gamma$  branching fraction in SUSY and the SM and test the decoupling limit, the electro-weak corrections to the SM  $\gamma\gamma$  decay width [30], which decrease the SM branching fraction by 2 to 3% in the mass interval  $90 < M_H < 140$  GeV and are not known for the MSSM, are removed.

## 2.1 Coupling suppression through SUSY corrections

The ratios of the  $h^0$  couplings to up-type quarks and gauge bosons to their SM values scale as  $\cos\alpha/\sin\beta$  and  $\sin(\beta - \alpha)$ , respectively, where  $\alpha$  is the mixing angle in the CP-even Higgs sector and depends on  $M_A$  for small to intermediate values of its mass. This induces a decrease of the couplings to top and  $W^\pm$ ,  $Z^0$  which propagates to the  $\sigma(gg \rightarrow h^0)$ ,  $h^0 \rightarrow \gamma\gamma$ ,  $W^+W^-$  and  $h^0 \rightarrow \gamma\gamma$ ,  $Z^0Z^0$  branching fractions.

At relatively high values of  $\tan\beta$  and for some values of the soft SUSY parameters which enter in radiative corrections for the Higgs sector, the coupling of the  $h^0$  boson to  $b$  quarks and  $\tau$  leptons becomes strongly suppressed. In the case of the  $h^0 b\bar{b}$  couplings, additional suppression could also occur as a result of vertex corrections involving gluino/sbottom loops.

In the decoupling regime, scalar top and, to a lesser extent, bottom contributions may still suppress the gluonic width and thus the  $gg \rightarrow h^0$  cross section as well as the  $h^0 \rightarrow \gamma\gamma$  decay branching fraction. This is important for light squark masses and large values of the mixing parameter in the stop sector,  $X_t$  [31–34].

Finally, at high  $\tan\beta$  and low  $M_A$  values, there is the so-called “intense coupling” regime [35] in which the three neutral Higgs bosons are very close in mass and have enhanced couplings to bottom quarks and tau leptons and thus, reduced branching ratios to  $W$  and  $Z$  bosons and to photons. Some points of the parameter space in which this scenario occurs, in particular at  $\tan\beta > 10$ , should be removed by the  $h^0, H^0, A^0 \rightarrow \tau\tau$  searches.

## 2.2 Rate suppression through decays to SUSY particles

Decays into pairs of SUSY particle, with mass smaller than  $M_{h^0}/2$ , modify the  $h^0$  branching fractions into SM particles. In practice there are two scenarios which are relevant to the reduction of the SM yields. If the LSP neutralino is light, the decay  $h^0 \rightarrow \tilde{\chi}^0 \tilde{\chi}^0$  may induce a large  $h^0$  invisible decay width and suppress its standard decays for some specific combinations of the  $M_1$ ,  $M_2$  and  $\mu$  parameters [33, 34, 36]. This scenario has received only some marginal attention [37, 38] so far<sup>1</sup>. It is now becoming an

intriguing possibility in view of the results by the DAMA, CoGENT and CRESST experiments, all reporting excess of events compatible with the interaction of a light WIMP with large scattering cross section on nucleons. We study this possibility with a dedicated scan where we restrict the parameter ranges to  $-120 < M_1 < 120$  GeV and  $-650 < M_2 < 650$  GeV. Detailed results on pMSSM scenarios compatible with the possible signal reported by the three experiments are given elsewhere [40]. Here, we do not consider the  $\tilde{\chi}p$  cross section as a constraint and study instead the modification of the Higgs branching fractions induced by decays into  $\tilde{\chi}_1^0$  pairs. The constraint from the

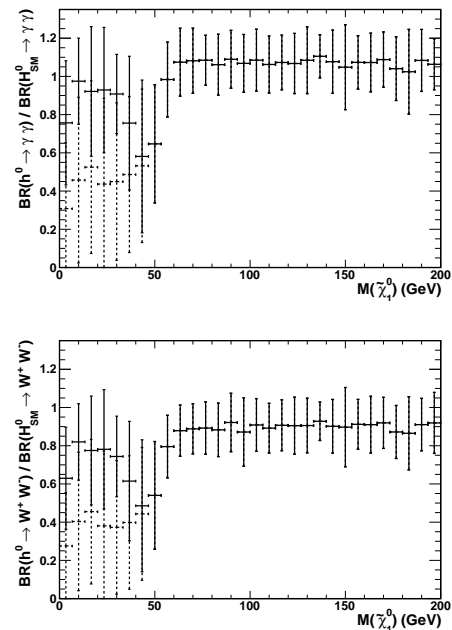


**Fig. 1.** The ratio of the branching fraction for  $h^0 \rightarrow \gamma\gamma$  (upper panel) and  $W^+W^-, Z^0Z^0$  (lower panel) to the SM prediction, obtained with HDECAY, as a function of the lightest neutralino mass for pMSSM points with  $A^0$  boson,  $\tilde{t}_1$  and  $\tilde{b}_1$  masses above 500 GeV. The dashed and full vertical bars give the full range of values for pMSSM points before and after applying the constraint on the  $Z^0$  invisible width, respectively.

$Z^0$  invisible decay width measured at LEP restricts the parameter space to points where the  $\tilde{\chi}_1^0$  is bino-like, if its mass is below 45 GeV, and thus to relatively large values of the higgsino mass parameter  $|\mu|$ . Since a large decay width into  $\tilde{\chi}_1^0 \tilde{\chi}_1^0$  corresponds to small values of  $|\mu|$ , this remove a large part of the parameter space where the invisible Higgs decay width is large. Still, we observe an important suppression of decays into  $\gamma\gamma$  and  $W^+W^-, Z^0Z^0$  for  $45 \text{ GeV} < M_{\tilde{\chi}_1^0} < M_{h^0}/2$  and  $|\mu| < 150$ , corresponding to a combination of parameters where the  $\tilde{\chi}_1^0$  is a mixed higgsino-gaugino state. In this region, the suppression reaches values up to a factor of five, which may upset the sensitivity of the LHC light Higgs searches in the canonical channels (see Figure 1). The second scenario has

<sup>1</sup> It has now been reconsidered in details in [39].

the lightest stau,  $\tilde{\tau}_1^\pm$ , below threshold for the  $h^0 \rightarrow \tilde{\tau}_1^+ \tilde{\tau}_1^-$  decay. In this case the decay into stau pairs almost saturates the  $h^0$  decay width and again suppresses the  $\gamma\gamma$  and  $WW/ZZ$  rates [41]. Since the  $M_{\tilde{\tau}_1} - M_{\tilde{\chi}_1^0}$  is small the  $h^0$  decay consists of two very soft  $\tau$  jets which would fail the trigger cuts at the LHC. However, this scenario is tightly constrained by the results of the LEP-2 searches.

### 3 Current and projected bounds

We consider four sets of constraints on SUSY parameters. These are from direct searches i) for SUSY particles with  $MET$  signatures and ii) for  $A^0$  bosons in the channel  $A^0 \rightarrow \tau^+ \tau^-$ , iii) from the  $B_s \rightarrow \mu^+ \mu^-$  rare decay and iv) from dark matter direct detection experiments. These constraints, originating from different sectors of the theory, are all sensitive to the SUSY parameters most relevant for setting the couplings and decay branching fractions of the light  $h^0$  bosons. Their combination provides the boundary conditions for the parameter space where we test the possible suppression of the yields in the LHC Higgs searches. We start from the situation outlined by the current data and project towards the status of these bounds at the time of the completion of the LHC run, for  $\sqrt{s}=7$  TeV, at the end of 2012, assuming no signal is observed, except for the  $B_s \rightarrow \mu^+ \mu^-$  decays, for which we assume a branching fraction equal to its SM expectation.

#### 3.1 Direct $\tilde{g}$ and $\tilde{q}$ searches at LHC

The direct searches for  $MET$  signatures with jets and leptons probe  $\tilde{g}$  and  $\tilde{q}$  masses up to  $\sim 500$  GeV with  $1 \text{ fb}^{-1}$  and  $\sim 750$  GeV with  $15 \text{ fb}^{-1}$  at 7 TeV [6–8]. LHC operation at 8 TeV for an integrated luminosity of  $15 \text{ fb}^{-1}$  will further push this sensitivity. While these are significantly constraining its parameter space, they are hardly decisive in disproving the MSSM as a viable theory. In fact, the gluino and squark masses can be pushed beyond those kinematically accessible in the current LHC run and still the MSSM would have all those features which have made SUSY so popular as SM extension, though at the cost of an increase of the fine tuning parameter.

Of special interest, in relation to the Higgs sector, are the constraint derived on the mass of the lightest scalar top,  $\tilde{t}_1$  quark. This squark is correlated with  $M_h$  and it can play a role together with the  $\tilde{b}_1$  in modifying the  $h^0$  couplings. Figure 2 shows the fractions of accepted pMSSM points which are compatible with the results of the CMS analyses in the fully hadronic [1] and in the leptonic channels [4, 5] on  $1 \text{ fb}^{-1}$  and its projection for  $15 \text{ fb}^{-1}$  at 7 TeV, as a function of the masses of the lightest squark of the first two generations  $\tilde{q}_{1,2}$  and of the  $\tilde{t}_1$ . These are obtained performing the same analysis as in [8]. In the upper left panel of Figure 2 we also present a first estimate of the improvement of the sensitivity to scalar quarks of the first two generation for 8 TeV LHC operation. From the results of generic scalar quark searches, which are not optimised

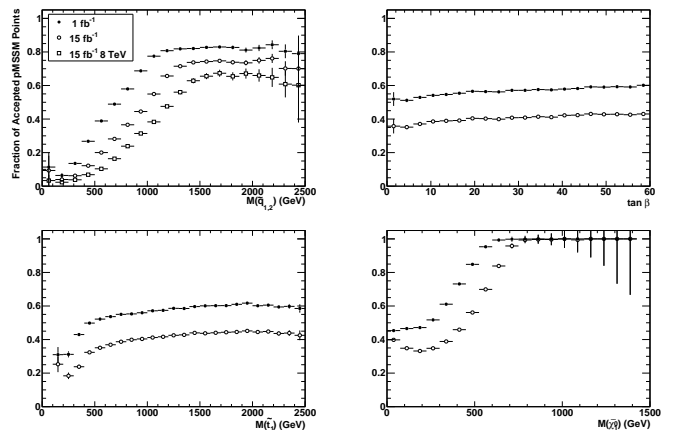


**Fig. 2.** Fraction of accepted pMSSM points not excluded by the SUSY searches on 1 (filled circles) and  $15 \text{ fb}^{-1}$  of LHC data at 7 TeV (open circles) and at 8 TeV (open squares) as a function of the mass of the lightest squark of the first two generations (upper left panel), of the mass of the scalar top  $\tilde{t}_1$  (lower left panel), of  $\tan \beta$  (upper right panel) and of the mass of the lightest neutralino  $\tilde{\chi}_1^0$  (lower right panel).

for  $\tilde{t}$ , and dedicated  $t\bar{t} + MET$  analyses, as that of ref. [42],  $15 \text{ fb}^{-1}$  of LHC data should be sensitive to MSSM solutions with light scalar quarks of the third generation with masses  $\sim 300\text{--}400$  GeV (see also [43]). Sensitivity beyond this mass limit is limited by the small production cross sections and the large backgrounds from top events. On the other hand, after removing pMSSM points excluded by the LHC searches, the acceptance w.r.t. other variables of interest here, such as  $M_A$  and  $\tan \beta$ , is flat, indicating that the gluino and scalar quark searches do not influence the Higgs sector parameters.

#### 3.2 Direct $A^0 \rightarrow \tau^+ \tau^-$ searches at LHC

The result of the direct search for the  $A^0$  boson at the LHC is the single most constraining piece of information on the  $(M_A, \tan \beta)$  plane. The CMS collaboration has presented the results of a search for neutral Higgs bosons decaying into  $\tau$  pairs based on  $1.1 \text{ fb}^{-1}$  of integrated luminosity [44] and recently reported a preliminary update based on the analysis of  $4.6 \text{ fb}^{-1}$  [10]. The search not revealing any significant excess of events, limits on the product of production cross section and decay branching fraction as a function of the boson mass, corresponding to the 95% C.L. expected bound are given in [45]. In order to map these bounds on the  $(M_A, \tan \beta)$  plane for the pMSSM and project them to  $15 \text{ fb}^{-1}$  of data, we compute the product of production cross section and decay branching fraction into  $\tau$  pairs for the  $A^0$  for each accepted pMSSM point. First we validate our procedure by taking the contour of the points having this product equal to that corresponding to the CMS expected limit. The right panel of Figure 3 shows this region for pMSSM points compared to the published CMS contour. These agree within 15%. Then, we

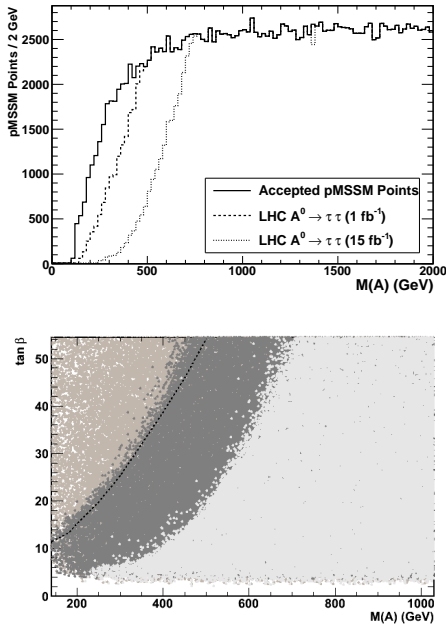


**Fig. 3.** Distribution of pMSSM points after the  $A^0 \rightarrow \tau^+\tau^-$  search projected on the  $M_A$  (upper panel) and  $(M_A, \tan\beta)$  plane (lower panel) for all accepted pMSSM points (medium grey), points not excluded with  $1 \text{ fb}^{-1}$  of data (dark grey) and the projection for the points not excluded with  $15 \text{ fb}^{-1}$  of data (light grey). The dashed line on the  $(M_A, \tan\beta)$  plot indicates the 95 % C.L. limit derived by CMS in the  $M_{h^0}$ -max scenario with  $M_{\text{SUSY}} = 1 \text{ TeV}$  for  $1.1 \text{ fb}^{-1}$ .

rescale the product to reproduce the projected limit for  $15 \text{ fb}^{-1}$  and remove the points which can be excluded if no signal is observed. Figure 3 shows the points surviving this selection in the  $M_A$  and  $(M_A, \tan\beta)$  parameter space. We note that the 2012 data should severely constrain the low  $M_A$  scenario by removing all solutions with  $M_A < 220 \text{ GeV}$  and restricting the region with  $M_A < 400 \text{ GeV}$  to  $\tan\beta$  values below 10. However, a tiny region with  $220 < M_A < 350 \text{ GeV}$  survives for  $\tan\beta \simeq 5$ .

### 3.3 $B_s^0 \rightarrow \mu^+\mu^-$ at LHC

The decay  $B_s \rightarrow \mu^+\mu^-$  is very sensitive to the presence of SUSY particles. At large  $\tan\beta$ , the SUSY contribution to this process is dominated by the exchange of neutral Higgs bosons, and very restrictive constraints can be obtained on the supersymmetric parameters [46]. Indeed, the couplings of the neutral Higgs bosons to  $b$  quark and muons are proportional to  $\tan\beta$ , which can lead to enhancement of orders of magnitude compared to the SM value, which is helicity suppressed.

The  $B_s \rightarrow \mu^+\mu^-$  decay has been searched for at the Tevatron and the LHC. The CDF experiment has reported an excess of events corresponding to a branching fraction of  $(1.8_{-0.9}^{+1.1}) \times 10^{-8}$  [47]. The LHCb and CMS collaborations did not observe any significant excess and re-

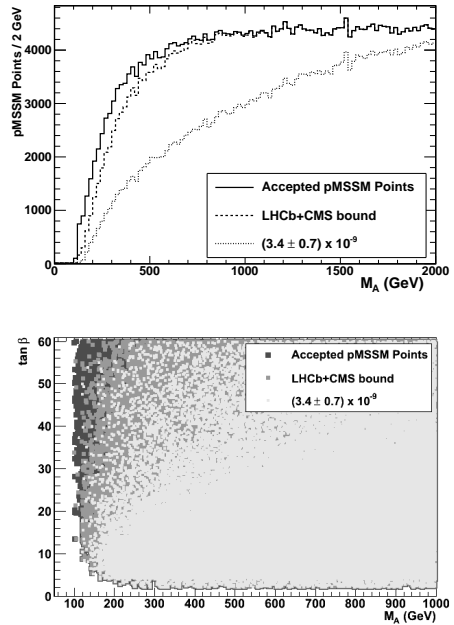


**Fig. 4.** Distribution of pMSSM points after the  $B_s \rightarrow \mu^+\mu^-$  constraint projected on the  $M_A$  (upper panel) and  $(M_A, \tan\beta)$  plane (lower panel) for all accepted pMSSM points (medium grey), points not excluded by the combination of the present LHCb and CMS analyses (dark grey) and the projection for the points compatible with the measurement of the SM expected branching fractions with a 20% total uncertainty (light grey).

leased a 95% C.L. combined limit of  $\text{BR}(B_s \rightarrow \mu^+\mu^-) < 1.1 \times 10^{-8}$  [48], which is only  $\sim 4$  times above the SM predictions. In order to take into account the theoretical uncertainties, in our numerical analysis we adopt the limit  $\text{BR}(B_s \rightarrow \mu^+\mu^-) < 1.26 \times 10^{-8}$ .

We compare our accepted pMSSM points to this limit as well as to the projected constraint in the case of observation of the decay with a SM-like rate of  $\text{BR}(B_s \rightarrow \mu^+\mu^-) = (3.4 \pm 0.7) \times 10^{-9}$ , to which we have attached a 20% total relative uncertainty, by the end of the 2012 run. The results are presented in Figure 4 in the  $M_A$  and  $M_A$ - $\tan\beta$  planes. The current limit affects the low  $M_A$  values up to 700 GeV, excluding large  $\tan\beta$  values, below  $M_A \sim 200 \text{ GeV}$ . The projected constraint has a stronger impact, with more than half of the spectrum being excluded for  $M_A \lesssim 700 \text{ GeV}$ . However, the low  $\tan\beta$  region at  $\tan\beta \sim 5$  remains largely unaffected also by this constraint.

### 3.4 Dark matter direct detection experiments

Dark matter direct detection experiments have made great progress exploring  $\tilde{\chi}p$  scattering cross sections in the range predicted by the MSSM [49, 50]. In particular, the recent XENON 100 result [50], places a 90% C.L. upper bound on the spin-independent  $\tilde{\chi}p$  cross section around  $10^{-8} \text{ pb}$  for  $M_{\text{WIMP}} \simeq 100 \text{ GeV}$  and excludes  $\simeq 20\%$  of the ac-

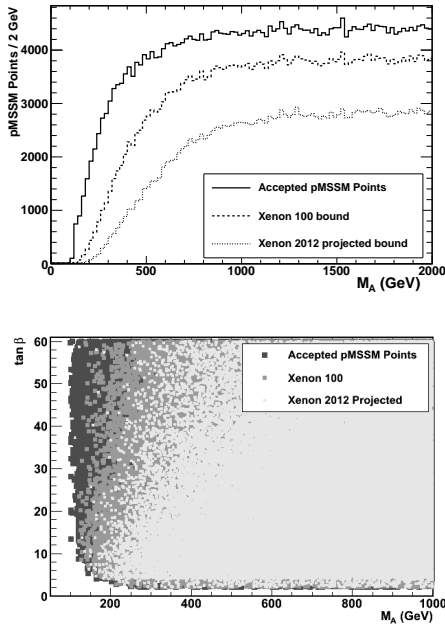


**Fig. 5.** Distribution of pMSSM points after the dark matter direct detection constraint projected on the  $M_A$  (upper panel) and  $(M_A, \tan \beta)$  plane (lower panel) for all accepted pMSSM points (medium grey), points not excluded by the current XENON-100 data (dark grey) and the projection for the XENON sensitivity at the end of 2012 (light grey).

cepted pMSSM points in our scan. By the end of 2012, this bound should be improved by a factor of 7, if no signal is observed, which will exclude  $\simeq 50\%$  of the accepted pMSSM scan points within our scan range. The  $\tilde{\chi}p$  spin-independent scattering process has contributions from scalar quark exchange and t-channel Higgs exchange [51]. The latter dominates over vast region of the parameter space with the Higgs coupling to the proton depending on its coupling to gluons, through a heavy quark loop and to non-valence quarks. The scattering cross section retains a strong sensitivity on the CP-odd boson mass as highlighted in Figure 5 which shows the pMSSM points retained after the XENON 100 and the projected 2012 sensitivity. The 2012 data should exclude virtually all solutions with  $M_A \lesssim 200$  GeV, independent on the value of  $\tan \beta$ , if no signal is detected.

## 4 The $h^0$ boson at LHC and MSSM constraints

The ATLAS and CMS experiments have recently combined the results of their searches for a SM-like Higgs boson on  $1.0\text{-}2.3 \text{ fb}^{-1}$  of statistics per experiment [52] obtaining a 95% C.L. upper limit on the ratio  $R_{ff} = \frac{\sigma \times \text{BR}(h^0 \rightarrow ff)}{\sigma_{\text{SM}} \times \text{BR}(H_{\text{SM}}^0 \rightarrow ff)}$  of 2.23 at  $M_H = 120$  GeV. Updated preliminary results of the individual searches based on almost  $5 \text{ fb}^{-1}$  of statistics, which have just been released, are sen-

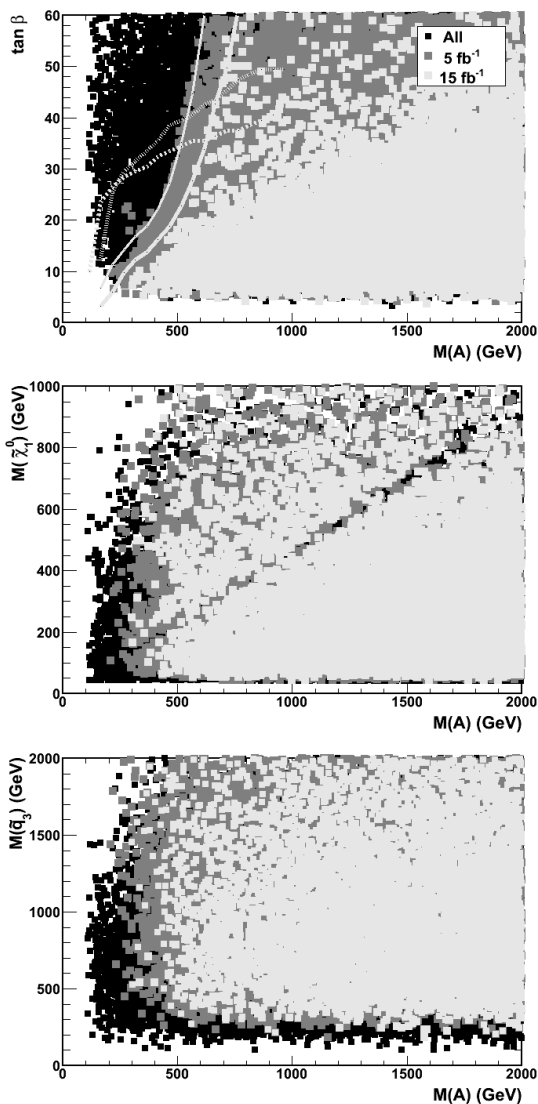
sitive to  $R \simeq 1$  and give possible hints of an excess in the number of events recorded by both experiments in several channels around a mass value of  $\sim 125$  GeV [10–12]. Here, we consider two distinct scenarios suggested by the 2011 LHC data and the constraints derived on the MSSM. First we consider the effect of the observation of a Higgs boson with a mass in the range  $123 < M_h < 127$  GeV, which corresponds to the case the reported excess would be confirmed by the 2012 data and where the upper end of the range represents the current 95% C.L. upper limit from LHC.

Alternatively, we study the scenarios with a significant suppression of the Higgs boson yield compared to the SM, corresponding to the exclusion of a SM-like Higgs boson. In both cases, the bounds on  $M_A$ ,  $\tan \beta$  and strongly interacting particles define the available parameter space for studying the  $h^0$  mass and the suppression of its couplings and thus the reduction of the yields in the LHC Higgs searches. We consider the two processes  $gg \rightarrow h^0 \rightarrow \gamma\gamma$  and  $gg \rightarrow h^0 \rightarrow W^+W^-, Z^0Z^0$ , which have the largest sensitivities in the present searches at the LHC.

### 4.1 Constraints from $M_h$ determination

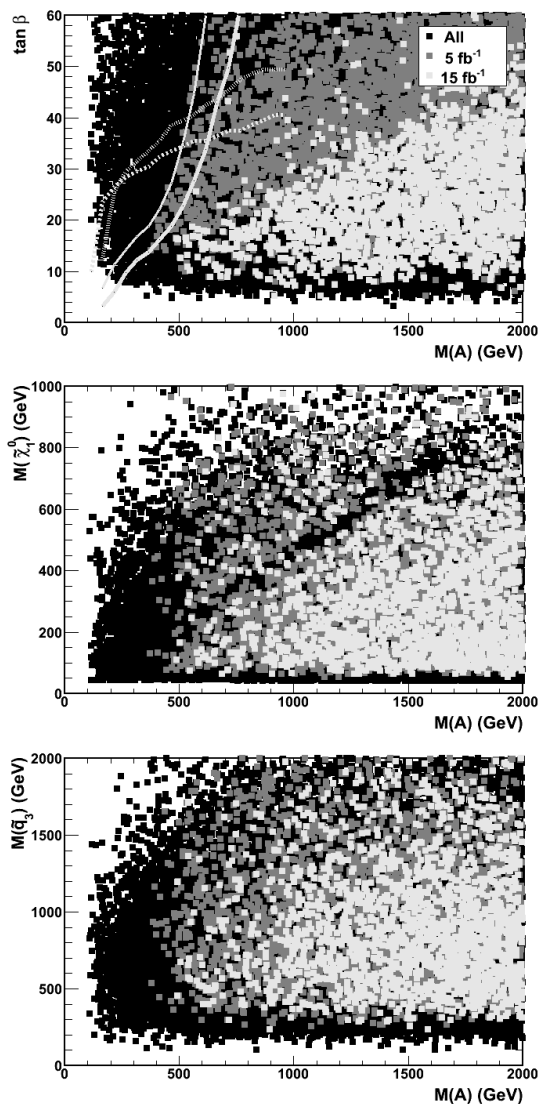
The determination of the mass of the lightest Higgs boson with an accuracy of order of 1 GeV places some significant constraints on the SUSY parameters, in particular in the typical mixing scenario, where its central value corresponds to a mass close to the edge of the range predicted in the MSSM. In order to evaluate these constraints, we select the accepted pMSSM points from our scans, which have  $123 < M_{h^0} < 127$  GeV. These are  $\simeq 20\%$  of the points not already excluded by the LHC SUSY searches with  $1 \text{ fb}^{-1}$  in our scan, where parameters are varied in the range given in the central column of Table 1.

Figure 6 shows the points fulfilling these conditions, which are also allowed by the other 2011 data constraints and by the 2012 projection. The parameter space is defined by three combinations of variables:  $M_A - \tan \beta$ ,  $M_A - M_{\tilde{\chi}_1^0}$  and  $M_A - M_{\tilde{q}_3}$ , where  $M_{\tilde{q}_3}$  is the minimum of the masses of the  $\tilde{t}_1$  and  $\tilde{b}_1$  squarks. We observe that imposing the value of  $M_{h^0}$  selects a broad wedge in the  $(M_A, \tan \beta)$  plane, at rather heavy  $A^0$  masses and moderate to large values of  $\tan \beta$  and extending beyond the projected sensitivity of the searches in the  $A^0 \rightarrow \tau^+\tau^-$  but also that of direct DM detection and would be compatible with a SM-like value for the rate of the  $B_s^0 \rightarrow \mu^+\mu^-$  decay. Next, we impose the condition that the yields in the  $\gamma\gamma$ ,  $W^+W^-$  and  $Z^0Z^0$  final states reproduce the observed rates of candidate events reported by the ATLAS and CMS collaborations. We require that  $1 \leq R_{\gamma\gamma} < 3$  and  $0.3 < R_{W^+W^-/Z^0Z^0} < 2.5$ . The points fulfilling these constraints are shown in Figure 7. Here, we observe that the wedge in the  $(M_A, \tan \beta)$  plane is further restricted and solutions with  $M_{\tilde{\chi}_1^0} > M_A$  are also strongly suppressed. The branching fractions for  $h^0 \rightarrow \gamma\gamma$  and  $h^0 \rightarrow W^+W^-$ , obtained with the HDECAY program, for the selected pMSSM points fulfilling the above mentioned constraints



**Fig. 6.** pMSSM points in the  $(M_A, \tan\beta)$  (top panel),  $(M_A, M_{\tilde{\chi}_1^0})$  (centre panel) and  $(M_A, M_{\tilde{q}_3})$ , where  $M_{\tilde{q}_3}$  is the minimum of the masses of the  $\tilde{t}_1$  and  $\tilde{b}_1$  squarks, (bottom panel) parameter space, giving  $123 < M_h < 127$  GeV. The different shades of grey show all the valid pMSSM points without cuts (black) and those fulfilling the Higgs mass cut allowed by the 2011 data (dark grey) and by the projected 2012 data (light grey), assuming no signal beyond the lightest Higgs boson is observed. The lines in the top plot show the regions which include 90% of the scan points for the  $A \rightarrow \tau^+\tau^-$  and  $B_s \rightarrow \mu^+\mu^-$  decays at the LHC and the dark matter direct detection at the XENON experiment, for the caption see Figure 10. The narrow corridor along the diagonal in the  $(M_A, M_{\tilde{\chi}_1^0})$  plane corresponds to the  $A^0$  funnel region where the  $\chi\chi \rightarrow A$  annihilation reduces  $\Omega_\chi h^2$  below the accepted range.

and with  $123 < M_h < 127$  GeV are shown in Figure 8. It is interesting to observe that a rather broad range of values are possible, depending on the SUSY parameters, but the ratios  $R_{\gamma\gamma}$  and  $R_{WW}$  are always highly correlated. In



**Fig. 7.** pMSSM points in the parameter planes  $(M_A, \tan\beta)$  (top panel),  $(M_A, M_{\tilde{\chi}_1^0})$  (centre panel) and  $(M_A, M_{\tilde{q}_3})$  (bottom panel), where  $M_{\tilde{q}_3}$  is the minimum of the masses of the  $\tilde{t}_1$  and  $\tilde{b}_1$  squarks, giving  $123 < M_h < 127$  GeV, after imposing the additional requirements on the Higgs rates. The color coding is the same as for Figure 6.

our pMSSM scans, we do not find solution where the  $\gamma\gamma$  yield is significantly enhanced compared to the SM while those in  $WW$  and  $ZZ$  are either unchanged or suppressed.

The effect of the Higgs constraints on some pMSSM parameters is shown in Figure 9, in terms of the fraction of valid pMSSM points, fulfilling the general requirements discussed in Section 2, those from searches by the end of 2012 and giving  $123 < M_h < 127$  GeV. In particular, a comparison of Figure 9 with Figure 2, which differ for the requirements on  $M_h$ , shows that values of  $\tan\beta \leq 6$  become disfavoured, while the masses of scalar quarks are not significantly affected. Imposing the condition that the yields in the  $\gamma\gamma$ ,  $W^+W^-$  and  $Z^0Z^0$  final states are con-

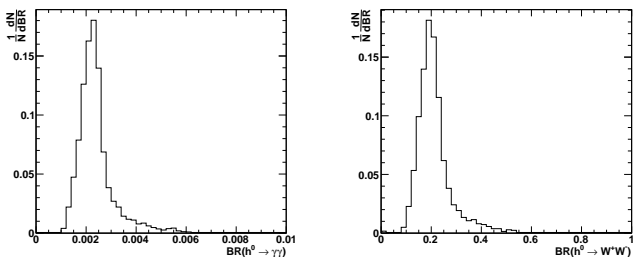


**Fig. 8.** Branching fractions for  $h^0$  decays into  $\gamma\gamma$  (left panel) and  $W^+W^-$  (right panel) pairs calculated with HDECAY for selected pMSSM points fulfilling the 2011 data constraints.

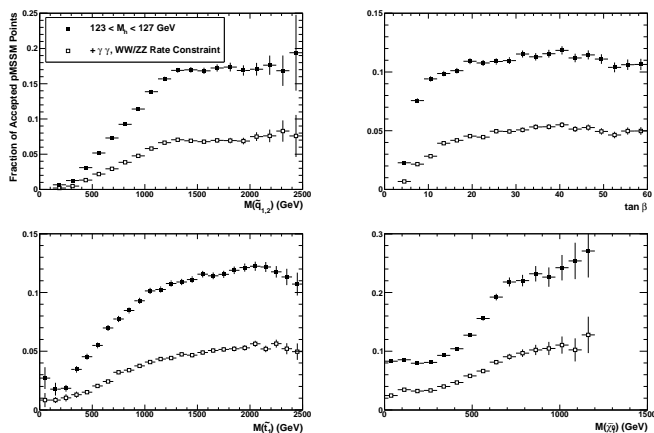


**Fig. 9.** Fraction of accepted pMSSM points, with  $123 < M_h < 127$  GeV (filled squares), not excluded by the SUSY searches with  $15 \text{ fb}^{-1}$  of 7 TeV data as a function of the mass of the lightest squark of the first two generations (upper left panel), of the mass of the scalar top  $\tilde{t}_1$  (lower left panel), of  $\tan\beta$  (upper right panel) and of the lightest neutralino  $\tilde{\chi}_1^0$  (lower right panel). The open square points show the fraction of pMSSM points after imposing the additional requirements on the Higgs rates.

sistent with the observed rates of candidate Higgs events reduces the fraction of accepted points preferentially at large masses of  $\tilde{t}_1$ ,  $\tilde{q}_{1,2}$  and  $\tilde{\chi}_1^0$ .

In order to estimate the effect of the program used for computing the  $h^0$  mass and decay branching fractions, we repeat the analysis using FeynHiggs and compare the results. We observe that 20.1% and 25.2% of the accepted pMSSM points in our scan have Higgs mass in the range  $123 < M_h < 127$  GeV using SoftSUSY and FeynHiggs, respectively. Of these 12% have  $R_{\gamma\gamma} \geq 1$  using HDECAY and 7.2% using FeynHiggs. Finally, we compute the fine tuning parameter  $\Delta$ , using the definition of ref. [9], for the points in the accepted Higgs mass range and for those having also the  $\gamma$ ,  $WW$  and  $ZZ$  rates within the constraints used above, and find that 20.6% and 18.4% of them have  $\Delta < 100$ .

## 4.2 Constraints from no Higgs observation

In this section, we turn to study the implications of a non-observation of the Higgs boson at the LHC. We select pMSSM points compatible with the current constraints and such that no signal beyond the SM is observed in the 2011 and 2012 statistics at LHC and XENON. Further, we request a rate suppression resulting in  $R_{\gamma\gamma}$  and  $R_{WW}$ ,  $R_{ZZ}$ , the ratio of the product  $\sigma \times \text{BR}$  to its SM expectations,  $\leq 0.3$  in the  $\gamma\gamma$  and  $WW$ ,  $ZZ$  channels. Such a suppression can be considered significant for the perspectives to discover, or exclude, a Higgs boson by the end of 2012.

Analysing the pMSSM points fulfilling this selection, we observe that three distinct classes of scenarios emerge: i) the region of the non-decoupling scenario with  $M_A < 250$  GeV and  $\tan\beta \sim 5$ , ii) the invisible Higgs scenario with  $M_{\tilde{\chi}_1^0} < M_{h^0}$  and small  $|\mu|$  and iii) the region with light  $\tilde{t}_1$ ,  $\tilde{b}_1$  squarks. These three scenarios are realised, respectively, in  $\sim 10^{-2}$ ,  $5 \times 10^{-4}$ , and  $4 \times 10^{-4}$  of the valid pMSSM points in our scans. The evolution of the parameter space for these scenarios after applying the constraints for  $5 \text{ fb}^{-1}$  of LHC data plus the current XENON 100 limit and the projected constraints for 2012 for  $15 \text{ fb}^{-1}$  of LHC data and the forthcoming XENON run are summarised in Figures 10 and 11, for  $\gamma\gamma$  and  $W^+W^-$ ,  $Z^0Z^0$ , using the combinations of parameters as in the previous section.

Class i) represents the tiny part of the low  $M_A$  and  $\tan\beta$  region left by  $A^0 \rightarrow \tau\tau$  and DM direct detection. Only  $\sim 8 \times 10^{-2}$  and  $7 \times 10^{-4}$  of the points in these region remain viable after applying the anticipated constraints from the LHC and XENON for the 2011 and 2012 data, respectively. In this region the decay  $H^0 \rightarrow Z^0Z^0$ , leading to the same final state as the SM Higgs process  $H_{SM}^0 \rightarrow Z^0Z^0$  [53, 54], is open. The results of the intermediate mass SM Higgs can be re-interpreted to place constraints on the low  $M_A$  scenario. We compare the product of cross section and decay branching fraction for  $gg \rightarrow H^0/A^0 \rightarrow Z^0Z^0$  to the LHC sensitivity for the SM Higgs decay into  $Z^0Z^0$ , rescaled by the assumed integrated luminosity. Figure 12 shows the regions of the  $(M_A, \tan\beta)$  plane where the  $H^0 \rightarrow Z^0Z^0$  rate exceeds the LHC sensitivity for 5 and  $15 \text{ fb}^{-1}$ . These cover part of the scenario i) parameter space left after the other constraints.

The light neutralino scenario (class ii)) may prove difficult to test directly in the squark and gluino sector due to the small transverse energy released. The dominant invisible Higgs decay, responsible for the yield suppression in the canonical channels, represents a distinct signature which should be feasible to test experimentally [38]. From our simulation we estimate that  $\sim 7 \times 10^{-2}$  of the points in this scenario should remain not excluded, after applying the constraints from the 2012 LHC and direct DM searches. Finally, for class iii) dedicated searches for stop and sbottom production and decay, involving  $t$  and  $b$ -tagging in events with jets and  $MET$  are already under way [55, 56], and will be further pursued to probe the mass region relevant for a possible Higgs rate suppression.



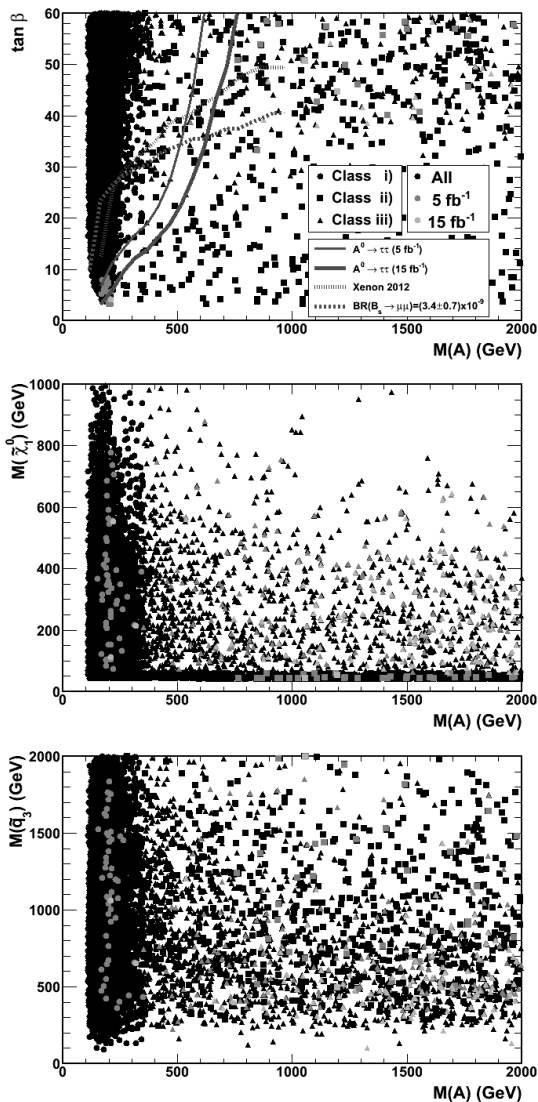


**Fig. 10.** pMSSM points in the  $(M_A, \tan \beta)$  (top panel),  $(M_A, M_{\tilde{\chi}_1^0})$  (centre panel) and  $(M_A, M_{\tilde{q}_3})$ , where  $M_{\tilde{q}_3}$  is the minimum of the masses of the  $\tilde{t}_1$  and  $\tilde{b}_1$  squarks (bottom panel) parameter space, giving a suppression of the  $gg \rightarrow h^0 \rightarrow \gamma\gamma$  rate compared to the SM prediction, corresponding to  $R_{\gamma\gamma} \leq 0.3$ . The different shades of grey show the points allowed in the pMSSM without cuts and those allowed by the 2011 data and by the projected 2012 data, assuming no signal is observed. The point shape gives the classification of the points depending on the relevant suppression mechanism, as discussed in the text. The lines in the top plot show the regions which include 90% of the scan points for the  $A \rightarrow \tau^+\tau^-$  and  $B_s \rightarrow \mu^+\mu^-$  decays at the LHC and the dark matter direct detection at the XENON experiment.

## 5 Conclusion

The Higgs boson searches at the LHC, in conjunction with those for  $B_s^0 \rightarrow \mu^+\mu^-$  again at the LHC and dark matter direct detection in underground experiments, place highly constraining bounds on the MSSM parameters. Inspired

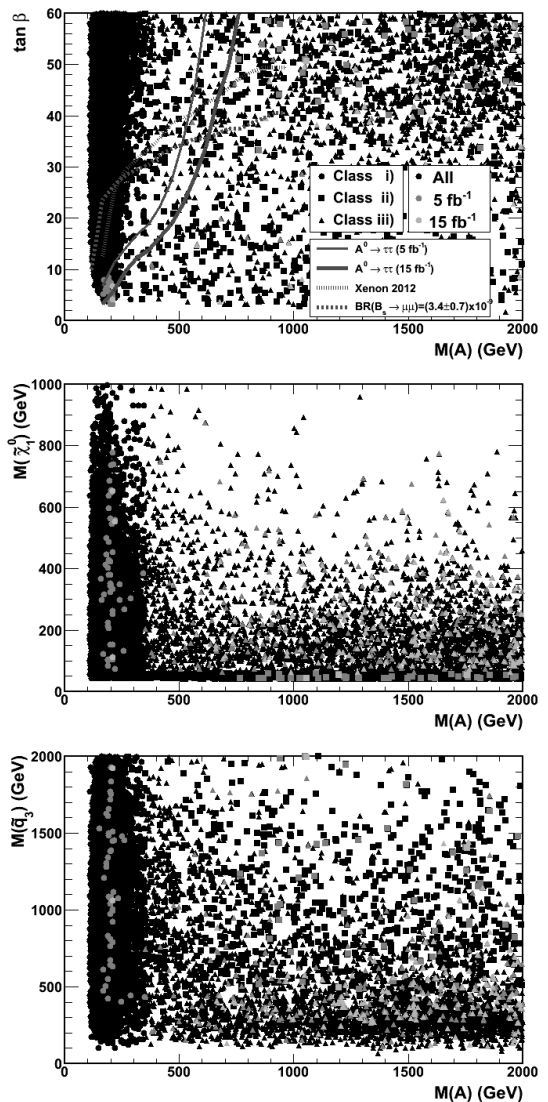


**Fig. 11.** pMSSM points in the  $(M_A, \tan \beta)$  (top panel),  $(M_A, M_{\tilde{\chi}_1^0})$  (centre panel) and  $(M_A, M_{\tilde{q}_3})$ , where  $M_{\tilde{q}_3}$  is the minimum of the masses of the  $\tilde{t}_1$  and  $\tilde{b}_1$  squarks (bottom panel) parameter space, giving  $R_{WW}, R_{ZZ} < 0.3$ . The symbol colour and shape coding is the same as in Figure 10.

by the preliminary results reported by the ATLAS, CMS and LHCb collaborations, we have analysed two scenarios. The first has a light Higgs boson, with mass  $123 < M_h < 127$  GeV, no signal from the  $MET$  searches and the  $B_s^0 \rightarrow \mu^+\mu^-$  decay with SM-like branching fraction. The second has no light Higgs boson within a factor of three from the SM rate and again no signal from strongly interacting particles and SM-like  $B_s^0 \rightarrow \mu^+\mu^-$  decay rate.

We perform flat scans of the 19-parameter pMSSM space imposing constraints from searches at LEP and the Tevatron, flavour physics and dark matter relic density. We observe that imposing the mass of the lightest Higgs boson in the range  $123 < M_h < 127$  GeV restricts the parameter space within a wedge in the  $(M_A, \tan \beta)$  plane,

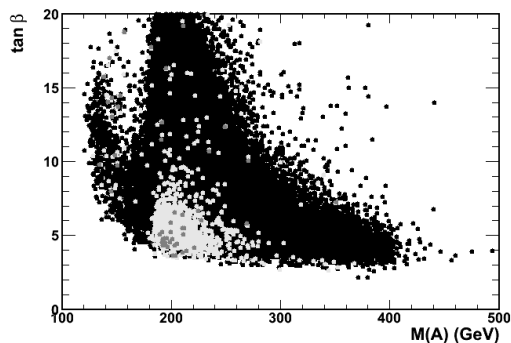


**Fig. 12.** pMSSM points in the  $(M_A, \tan \beta)$  plane with rate for  $bb \rightarrow H^0/A^0$ ,  $gg \rightarrow H^0/A^0$ ;  $H^0/A^0 \rightarrow Z^0 Z^0$  non-zero (black points) and exceeding the expected sensitivity to  $Z^0 Z^0$  final states from the  $H^0_{SM}$  search for 5 (medium grey) and  $15 \text{ fb}^{-1}$  (light grey) of integrated luminosity.

corresponding to rather large values of the  $A^0$  mass and moderate to large values of  $\tan \beta$ , while it does not significantly affect the values of the masses of weakly interacting supersymmetric particle partners. Further imposing that the yields in the  $\gamma\gamma$ ,  $W^+W^-$  and  $Z^0 Z^0$  final states reproduce the rates of candidate events reported by the ATLAS and CMS collaborations the wedge in the  $(M_A, \tan \beta)$  plane becomes more pronounced and the fraction of accepted points gets reduced preferentially at large masses of  $\tilde{t}_1$ ,  $\tilde{q}_{1,2}$  and  $\tilde{\chi}_1^0$ .

On the contrary, a non-observation of the Higgs boson, corresponding to a suppression of its yields in the  $\gamma\gamma$ ,  $WW$  and  $ZZ$  final states to a factor of  $\simeq 3$  compared to the SM expectations, would confine the viable sets of MSSM parameters to just three narrow regions having light  $A^0$  and low  $\tan \beta$  values,  $M_{\tilde{\chi}_1^0} < M_h^0$  and invisible  $h^0$  decays or light  $\tilde{t}_1$ ,  $\tilde{b}_1$  scalar quarks. Each of these scenarios consists of a tiny fraction of the valid pMSSM points and can be independently probed, through a direct search for the  $A^0$  and  $H^0$  Higgs states, light neutralinos and invisible Higgs decays and light to intermediate mass scalar top quarks. While it is still too early to draw definite conclusions from the preliminary LHC results, the continuation of all these searches at the LHC and dark matter experiments should provide us with a definite test of the MSSM independent on the mass scales of the scalar quarks of the first two generations and of the gluino.

## Acknowledgements

We would like to thank M. Mangano for supporting this activity and the LPCC for making dedicated computing resources available to us. We are grateful to Abdelhak Djouadi for extensive discussion and his suggestions. We also acknowledge useful discussions with G. Belanger, M. Spira and S. Heinemeyer. Several colleagues in the LHC collaborations provided us with valuable feedback, in particular A. De Roeck and B. Hooberman. We are grateful to E. Gianolio for computing support and to E. Aprile,

P. Beltrame and A. Melgarejo for providing us with information on the current and expected sensitivity of the XENON experiment.

## References

1. S. Chatrchyan, et al. (CMS Collaboration), Phys. Rev. Lett. **107**, 221804 (2011), [arXiv:1109.2352](#).
2. G. Aad, et al. (ATLAS Collaboration) (2011), [arXiv:1109.6572](#).
3. G. Aad, et al. (ATLAS Collaboration) (2011), [arXiv:1110.6189](#).
4. CMS Collaboration (2011), CMS-PAS-SUS-11-010.
5. CMS Collaboration (2011), CMS-PAS-SUS-11-011.
6. J. A. Conley, J. S. Gainer, J. L. Hewett, et al. (2011), [arXiv:1103.1697](#).
7. S. Sekmen, S. Kraml, J. Lykken, et al. (2011), [arXiv:1109.5119](#).
8. A. Arbey, M. Battaglia, F. Mahmoudi, Eur. Phys. J. **C72**, 1847 (2012), [arXiv:1110.3726](#).
9. M. Perelstein, C. Spethmann, JHEP **04**, 070 (2007), [hep-ph/0702038](#).
10. F. Gianotti, G. Tonelli, Talks given at the CERN seminar on update on the Standard Model Higgs searches, CERN, 13/12/2011; <https://indico.cern.ch/conferenceDisplay.py?confId=164890>.
11. ATLAS Collaboration (2012), CERN-PH-EP-2012-019 [arXiv:1202.1408](#) [[hep-ex](#)].
12. CMS Collaboration (2012), CERN-PH-EP-2012-023 [arXiv:1202.1488](#) [[hep-ex](#)].
13. A. Djouadi, et al. (1998), [hep-ph/9901246](#).
14. M. S. Carena, M. Quiros, C. E. M. Wagner, Nucl. Phys. **B461**, 407 (1996), [hep-ph/9508343](#).
15. S. Heinemeyer, W. Hollik, G. Weiglein, Phys. Lett. **B440**, 296 (1998), [hep-ph/9807423](#).
16. M. S. Carena, et al., Nucl. Phys. **B580**, 29 (2000), [hep-ph/0001002](#).
17. A. Arbey, M. Battaglia, A. Djouadi, et al., Phys. Lett. **B708**, 162 (2012), [arXiv:1112.3028](#).
18. M. S. Carena, S. Heinemeyer, C. E. M. Wagner, et al., Eur. Phys. J. **C26**, 601 (2003), [hep-ph/0202167](#).
19. B. C. Allanach, Comput. Phys. Commun. **143**, 305 (2002), [hep-ph/0104145](#).
20. A. Djouadi, J. Kalinowski, M. Spira, Comput. Phys. Commun. **108**, 56 (1998), [hep-ph/9704448](#).
21. S. Heinemeyer, W. Hollik, G. Weiglein, Comput. Phys. Commun. **124**, 76 (2000), [hep-ph/9812320](#).
22. S. Heinemeyer, W. Hollik, G. Weiglein, Eur. Phys. J. **C9**, 343 (1999), [hep-ph/9812472](#).
23. M. Muhlleitner, A. Djouadi, Y. Mambrini, Comput. Phys. Commun. **168**, 46 (2005), [hep-ph/0311167](#).
24. F. Mahmoudi, Comput. Phys. Commun. **178**, 745 (2008), [arXiv:0710.2067](#).
25. F. Mahmoudi, Comput. Phys. Commun. **180**, 1579 (2009), [arXiv:0808.3144](#).
26. A. Arbey, F. Mahmoudi, Comput. Phys. Commun. **181**, 1277 (2010), [arXiv:0906.0369](#).

27. G. Belanger, F. Boudjema, A. Pukhov, et al., *Comput. Phys. Commun.* **180**, 747 (2009), [arXiv:0803.2360](#).
28. M. Spira, A. Djouadi, D. Graudenz, et al., *Nucl. Phys.* **B453**, 17 (1995), [hep-ph/9504378](#).
29. M. Spira, *Nucl. Instrum. Meth.* **A389**, 357 (1997), [hep-ph/9610350](#).
30. G. Passarino, C. Sturm, S. Uccirati, *Phys. Lett.* **B655**, 298 (2007), [arXiv:0707.1401](#).
31. A. Djouadi, V. Driesen, W. Hollik, et al., *Eur. Phys. J.* **C1**, 149 (1998), [hep-ph/9612362](#).
32. A. Djouadi, *Phys. Lett.* **B435**, 101 (1998), [hep-ph/9806315](#).
33. A. Djouadi, *Phys. Rept.* **459**, 1 (2008), [hep-ph/0503173](#).
34. A. Djouadi, *Phys. Rept.* **457**, 1 (2008), [hep-ph/0503172](#).
35. E. Boos, A. Djouadi, M. Muhlleitner, et al., *Phys. Rev.* **D66**, 055004 (2002), [hep-ph/0205160](#).
36. A. Djouadi, M. Drees, P. Fileviez Perez, et al., *Phys. Rev.* **D65**, 075016 (2002), [hep-ph/0109283](#).
37. D. Cavalli, A. Djouadi, K. Jakobs, et al. (2002), [hep-ph/0203056](#).
38. R. Kinnunen, S. Lehti, A. Nikitenko, et al., *J. Phys.* **G31**, 71 (2005), [hep-ph/0503067](#).
39. D. Vasquez, G. Belanger, R. Godbole, et al. (2011), [arXiv:1112.2200](#).
40. A. Arbey, M. Battaglia, F. Mahmoudi, in preparation.
41. A. Djouadi, *Mod. Phys. Lett.* **A14**, 359 (1999), [hep-ph/9903382](#).
42. G. Aad, et al. (ATLAS), *Phys. Rev. Lett.* **108**, 041805 (2012), [1109.4725](#).
43. M. Papucci, J. T. Ruderman, A. Weiler (2011), [arXiv:1110.6926](#).
44. S. Chatrchyan, et al. (CMS Collaboration), *Phys. Rev. Lett.* **106**, 231801 (2011), [arXiv:1104.1619](#).
45. CMS Collaboration (2011), [CMS-PASHIG-11-009](#).
46. A. Akeroyd, F. Mahmoudi, D. Martinez Santos, *JHEP* **1112**, 088 (2011), [arXiv:1108.3018](#).
47. T. Aaltonen, B. Álvarez González, S. Amerio, et al. (CDF Collaboration), *Phys. Rev. Lett.* **107**, 191801 (2011).
48. CMS and LHCb Collaborations (2011), [LHCb-CONF-2011-047](#), [CMS-PAS-BPH-11-019](#).
49. Z. Ahmed, et al. (The CDMS-II Collaboration), *Science* **327**, 1619 (2010), [arXiv:0912.3592](#).
50. E. Aprile, et al. (XENON 100 Collaboration), *Phys. Rev. Lett.* (2011), [arXiv:1104.2549](#).
51. G. Jungman, M. Kamionkowski, K. Griest, *Phys. Rept.* **267**, 195 (1996), [hep-ph/9506380](#).
52. ATLAS and CMS Collaborations (2011), [ATLAS-CONF-2011-157](#), [CMS-PAS-HIG-11-023](#).
53. G. Aad, et al. (ATLAS Collaboration), *Phys. Lett.* **B705**, 435 (2011), [arXiv:1109.5945](#).
54. CMS Collaboration (2011), [CMS-PAS-HIG-11-015](#).
55. ATLAS (2011), [ATLAS-CONF-2011-098](#).
56. CMS (2011), [CMS-PAS-SUS-11-006](#).